Hindawi
Wireless Communications and Mobile Computing
Volume 2020, Article ID 8876669, 10 pages
https://doi.org/10.1155/2020/8876669

Research Article

RO-RAW: Run-Time Restricted Access Window Optimization in IEEE 802.11ah Network with Extended Kalman Filter

Zhao Liu and Peng Lv

The School of Computer and Communication Engineering, University of Science and Technology Beijing, Beijing, China

Correspondence should be addressed to Peng Lv; b1901775@ustb.edu.cn

Received 1 August 2020; Revised 16 September 2020; Accepted 29 September 2020; Published 21 October 2020

Academic Editor: Chaoyun Song

In 2016, the IEEE task group ah (TGah) published a new standard IEEE 802.11ah, aimed at providing network connectivity among a large number of Internet of Things (IoT) devices. Restricted access window (RAW) is one of the fundamental MAC mechanisms of IEEE 802.11ah. It reduces the contention overhead in the dense wireless environment by dividing stations into different RAW groups. However, how to optimize the RAW parameters is still an open issue, especially in the run-time environment. In this paper, we propose a run-time RAW optimization scheme, namely RO-RAW, to improve the performance of RAW in the IEEE 802.11ah networks. RO-RAW adopts the Extended Kalman Filter method to estimate the channel status and adjusts the RAW parameters according to the number of competing stations in real-time. The evaluation via NS-3 simulations shows that, by tuning the RAW parameters appropriately, RO-RAW substantially improves throughput, latency, and packet loss performance compared with another RAW optimization scheme in different simulation scenarios. The results further show that, when the channel is relatively congested, RO-RAW improves the RAW performance more significantly.

1. Introduction

Smart manufacturing [1, 2] and Industry 4.0 production environments modernize the traditional plants and factories. To remain competitive, several intelligent applications need to be deployed to upgrade the current plants, such as remote operation and maintenance [3], flexible production [4], and AI manufacturing automation [5]. To provide a better support for these applications, the industrial wireless network should also be deployed as the communication infrastructure. Compared with the traditional wired industrial communication systems, choosing wireless networks is a better option because it is easy to maintain and cost-effective.

Wireless local area networks (WLANs) have become the most popular and widely deployed networks. Thus, it is a good candidate for different industrial wireless applications with various requirements [6, 7]. In 2016, a new Wi-Fi standard named IEEE 802.11ah was released [8], which targets low-power and large-scale Internet of Things (IoT) network scenarios, including industrial IoT. IEEE 802.11ah has a transmission range up to 1 km with the advent of sub-GHz technologies and supports up to 8192 nodes in a WLAN. On the Media Access Control (MAC) layer, the most important issue is to increase the efficiency when a large number of energy-constrained stations deployed densely. Thus, several novel MAC mechanisms are introduced, such as short MAC header, Restricted Access Window (RAW), Target Wake Time (TWT), and Traffic Indication Map (TIM) segmentation.

The RAW mechanism is aimed at addressing the collision problem in a dense wireless network, where a large number of nodes are associated with a single access point (AP). The basic idea of the RAW mechanism is to divide stations into groups, and the stations in one group are only permitted to access the channel during a specific time slot. Thus, the collision probability is highly reduced by limiting the number of stations which simultaneously access the channel. However, the hierarchical RAW mechanism has several parameters to be adjusted, including the number of RAW slots, the duration of each RAW slot, and the RAW period, which are not defined in the standard. In order to obtain a better network performance, these parameters must be considered

jointly according to the channel status. In fact, there are already some related works [9–11] which provide the relationship between the parameter settings and the performance metrics (throughput, average latency, transmission success probability, etc.). But, the dynamicity of the channel contention status is rarely considered in these models, which could be a key factor affecting the network performance.

In this paper, the authors propose a run-time RAW optimization scheme, namely, RO-RAW, which adaptively optimizes the network performance by adjusting the RAW parameters according to the channel status. It first estimates the current channel status and returns the estimated station numbers by the Extended Kalman Filter (EKF) method. Based on the estimated number of competing stations, RO-RAW adjusts the RAW parameters to the optimal parameter settings which are calculated in advance corresponding to the number of stations. The main contributions of this paper are summarized as follows:

(i) We propose a run-time RAW parameter optimization scheme RO-RAW, which adaptively adjusts the RAW parameters to the theoretical optimal values based on the channel status

(ii) In order to estimate the channel status, we adopt the Extended Kalman Filter method to obtain the current competing stations. We clearly provide the system state equations of the 802.11ah networks and the way to measure the number of stations. Then, the estimated channel status can be easily obtained by iteration using EKF

The remainder of the paper is organized as follows. Section 2 reviews related work and the background on this research. Section 3 presents the proposed run-time RAW optimization scheme in detail. Section 4 shows the simulation results of the proposed scheme in detail. Finally, the conclusions are given in Section 5.

2. Background

2.1. IEEE 802.11 DCF and EDCA. IEEE 802.11ah inherits the most basic features of IEEE 802.11 MAC, such as distributed coordination function (DCF) and Enhanced Distributed Channel Access (EDCA). DCF is the fundamental MAC mechanism of the IEEE 802.11 family. It is a simple and flexible scheme to share the wireless medium among multiple stations. In DCF (Figure 1), stations adopt the Carrier Sense Multiple Access mechanism with Collision Avoidance (CSMA/CA) to contend for the channel access opportunity. Before a new transmission, each station must monitor the state of the wireless medium. If the medium is found idle for a DCF Interframe Space (DIFS) duration, the station is permitted to transmit its data. Otherwise, the transmission procedure must be frozen until the channel is sensed idle again. When the transmission of a station fails due to the collision or bit error, DCF adopts the Binary Exponential Backoff (BEB) algorithm to look for the next transmission opportunity [12]. The backoff duration is composed of several time slots, and the number of backoff slot value is selected randomly from $[0, CW - 1]$, where CW is the contention window size. In the initialization phase, CW is set to the minimal value (CW_{min}). Once the CW increases to the maximum value (CW_{max}), it is maintained at CW_{max} even if the next transmissions are still failed. After a successful data transmission, the CW is set back to CW_{min}.

In the IEEE 802.11e standard, a new channel access mechanism called EDCA is proposed to provide priority-based differentiated QoS. As shown in Figure 2, there are four access categories (AC) defined in EDCA, namely, voice (AC_VO), video (AC_VI), best-effort (AC_BE), and background (AC_BK). By differentiating the backoff parameters, high-priority traffic is able to transmit with a higher transmission chance than the low-priority traffic. Specifically, high-priority traffic uses shorter arbitration inter-frame space (AIFS), which is the interval that a frame needs to wait before it is transmitted. The size of the contention window is also set according to the priority of each kind of AC.

2.2. IEEE 802.11ah RAW Mechanism. The IEEE 802.11ah standard allows up to 8192 stations to associate with an AP, which is a highly attractive feature for a lot of IoT use cases. However, how to mitigate collisions and improve performance in such dense IoT networks is an urgent problem to be solved. Among the new mechanisms in 802.11ah, RAW is the core mechanism aimed at enabling fair channel access for a large number of stations and avoiding too many stations contending for channel access simultaneously. In this mechanism, the channel time is divided into several intervals, namely, the RAW periods and the shared channel access periods. Only the RAW stations from a specific group are allowed to access the channel and transmit in their corresponding RAW period. On the contrary, all stations are permitted to contend the channel in the shared channel access periods. The example of the different periods in RAW mechanism is shown in Figure 3.

For each AP, it broadcasts a beacon frame carrying a RAW Parameter Set (RPS), which specifies the RAW parameter configurations. Stations retrieve the RAW information from the beacon frame and access the channel in their corresponding RAW slot. The RPS information specifies the RAW related information, such as the RAW group, group start time, the number of RAW slots, and slot duration. The RAW slot duration is determined as follows:

$$D = 500\mu s + C \times 120\mu s. \quad (1)$$

In equation (1), D stands for the RAW slot duration, and C is the slot duration count subfield. Another parameter called the slot format subfield determines the number of RAW slots and C. If the slot format subfield is filled with 1, a single RAW period is composed of at most eight RAW slots and the maximum value of C is 2047; the duration of each slot is up to 246.14 ms. Otherwise, a RAW period is composed of at most 64 RAW slots and the maximum value of C is 255, and the duration of each

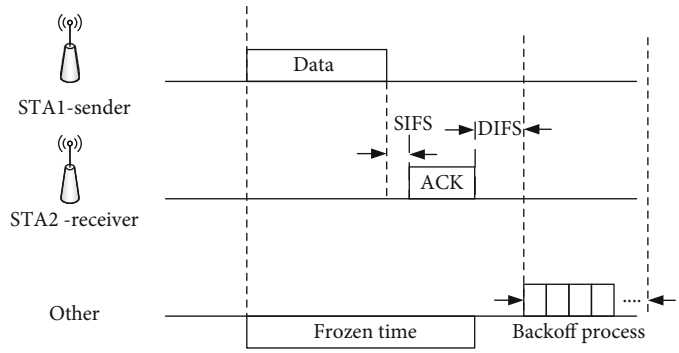

Figure 1: IEEE 802.11 DCF.

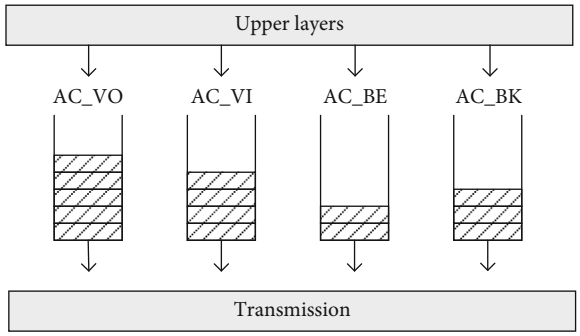

Figure 2: IEEE 802.11 EDCA.

slot is limited to 31.1 ms. The RAW stations are mapped to these slots according to the following rule:

$$i_{\text{slot}} = (x + N_{\text{offset}}) \bmod N_{\text{RAW}}. \quad (2)$$

In equation (2), i_{slot} represents the index of the RAW slot which the station is mapped. N_{RAW} is the number of slots predefined in one RAW period. N_{offset} is the offset value in the mapping function, and x is the index of the station.

The RPS also has a subfield called cross-slot boundary (CSB), which determines whether the stations are allowed to continue their transmissions when the current RAW slot ends. If CSB is set to 1, the stations can continue transmitting even though their RAW slot ends. Otherwise, stations should not trigger a transmission if the transmissions cannot be finished in the current RAW slot.

The backoff mechanism in RAW is also different to some extent compared with the previous IEEE 802.11 standards. Each station uses two kinds of backoff states of EDCA to manage data transmission inside and outside its allocated RAW slots. The first backoff state is used outside the RAW period, in which all stations contend for the channel freely. The stations in the first backoff state freeze their backoff timer at the beginning of each RAW period and resume the backoff timer at the end of the RAW period. On the contrary, the second backoff state is used inside the RAW period, where only the designated group of stations are allowed to contend for the channel. The stations in the second backoff state start to backoff inside their own RAW slot and discard the backoff state when their RAW slot ends.

2.3. Related Work on RAW Mechanism Optimization. Although the IEEE 802.11ah standard was published in 2016, research on IEEE 802.11ah has been conducted for more than five years. A few articles [11, 13–16] introduce a high-level overview of the core PHY/MAC mechanisms in IEEE 802.11ah and describe the advantages and challenges when designing these schemes. As one of the key technologies in IEEE 802.11ah, the RAW mechanism has been widely studied in many aspects. The work focusing on RAW analysis and optimization is more relevant to the research presented in this paper.

Several studies have been conducted to model and optimize the RAW parameter configuration in different network and traffic conditions. Raeesi et al. [9] propose an analytical model to derive the IEEE 802.11ah network performance, including throughput and energy consumption. It also shows the advantage of the RAW mechanism in throughput and delay compared with the basic scheme. In [10], the authors propose an analytical approach to investigate the RAW mechanism. Based on the analytical model, the paper provides the time distribution of the successful transmission by a Markov model. In [17], the authors provide a RAW enhancement scheme in the machine-to-machine scenario. The proposed scheme determines the optimal size of RAW by estimating the number of devices for the uplink access. However, the works mentioned above either only conduct a basic analytical model under a certain circumstance or provide a basic RAW optimization scheme with a simple channel sensing method, which may not be enough to reflect the real channel status. This will cause the network performance deviating from the calculated optimal value. In [18], the author proposes an adaptive RAW optimization scheme called CA-CWA. It estimates the channel state and adjusts the channel contention parameters to improve the real-time performance of the IEEE 802.11ah network. However, CA-CWA only considers and adapts the contention window to improve the RAW performance. Other RAW parameters, such as RAW slot duration and RAW slot number, are not considered and optimized. In this paper, the authors provide RO-RAW to adaptively adjust the IEEE 802.11ah RAW parameters in the run-time environment. Based on the

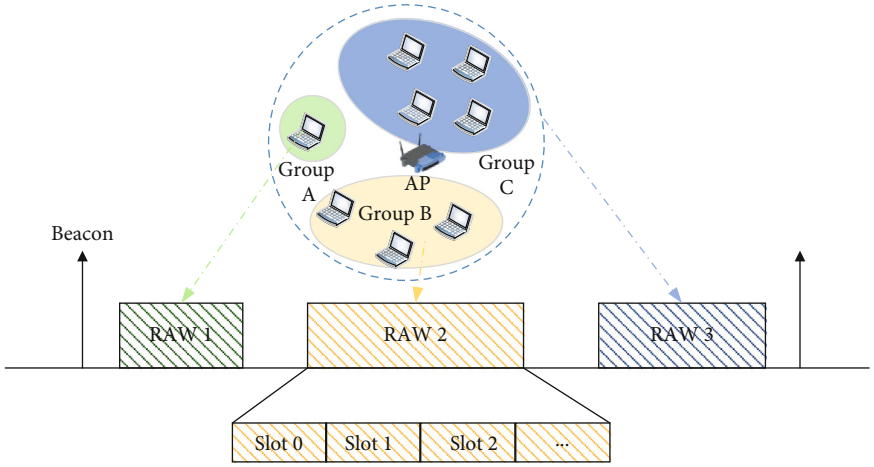

Figure 3: IEEE 802.11ah RAW mechanism.

estimated number of competing stations, RO-RAW is able to adjust RAW parameters in time to ensure the performance of RAW.

3. RAW Mechanism Optimization with Extended Kalman Filter

In this section, we introduce the system model and the RAW optimization problem first and subsequently provide a detailed description of the proposed RO-RAW. RO-RAW is a run-time adaptive scheme to improve the performance of the RAW mechanism. It adjusts the RAW parameters to the optimal parameter settings based on the estimated number of competing stations. Table 1 provides an overview of the variables used in the description of the system model and RO-RAW.

3.1. System Model. In this paper, we only consider a single wireless cell with a star topology. Assuming the wireless network has a total number of N nodes, each node supports the RAW mechanism defined in the IEEE 802.11ah standard. According to the RAW mechanism definition introduced in Section 2.2, if there are M RAW station groups, and the number of stations in ith group is G_i, we can have the following equations:

$$N = \sum_{i=1}^{M} G_i. \tag{3}$$

Because each group of stations monopolizes its allocated RAW period, in a certain group i in RAW period i, if there are r_i RAW slots in the RAW period, the number of stations in a RAW slot N^i_{RAW} is:

$$N^i_{\mathrm{RAW}} = G_i / r_i. \tag{4}$$

In each RAW slot, the stations still adopt basic DCF to compete for transmission. According to the Bianchi [19] model, let p be the probability that a transmitted packet collides with others in the RAW slot, and τ be the probability that a station transmits in a random slot time; we can obtain the following equations:

$$p = 1 - (1 - \tau)^{n-1}, \tag{5}$$

$$\tau = \frac{2(1-2p)}{(1-2p)(W+1) + pW(1-(2p)^m)}, \tag{6}$$

where W is the minimal contention window size and m is the retry limit. Both values are the predefined constant backoff parameters. From equation (5) and equation (6), we obtain the number of current competing stations in the RAW slot:

$$n = y(p) = 1 + \frac{\log(1-p)}{\log\left(1 - \left((2(1-2p))/(1-2p)(W+1) + pW(1-(2p)^m)\right)\right)} < N^i_{\mathrm{RAW}}. \tag{7}$$

Besides, the network throughput S is calculated as:

$$S = \frac{P_s P_{tr} L}{(1-P_{tr})\sigma + P_{tr} P_s T_s + P_{tr}(1-P_s) T_c}, \tag{8}$$

where

$$P_s = \frac{n\tau(1-\tau)^{n-1}}{1-(1-\tau)^n}, \qquad P_{tr} = 1 - (1-\tau)^n. \tag{9}$$

L is the average packet length. From the above derivations, it is obvious that the throughput is a function of the competing station number n. Since other variables in equation (8) are constant values, it exists the optimal value of n, which achieves the maximum throughput [20, 21]. The optimal value is easy to be obtained from equation (8) by calculating the derivative (equation (10)). Here we use n_{opt} to represent the optimal station number.

$$\frac{dS}{dn} = 0. \tag{10}$$

Table 1: Summary of the main notations and abbreviations.

Notation	Description
N	The total number of stations
M	The number of RAW station groups
G_i	The number of stations in ith group
N^i_{RAW}	The number of stations in ith RAW slot
r_i	The RAW slot number in a RAW
p	Transmission collision probability
τ	The transmission probability in a random slot time
L	The average packet length
T_c	The number of busy slots
T_p	The number of collision slots
$\hat{n}_k$	The estimated value of n at time k
K_k	Kalman gain
Q_k	Variance of random variable u_k
R_k	Variance of random variable v_k

1: **Step 1:** Initialize all the network and algorithm parameters.
2: **Step 2:** Compute the optimal station numbers n_{opt}.
3: **Step 3:** After the network has been initialized and running normally, each station calculates the current channel status $\hat{n}^i_k$ by the method introduced in Section 3.2 for ith RAW slot at time k.
4: **Step 4:** If $\hat{n}^i_k$ is beyond the value of n_{opt} for a period T_p, $n_{\mathrm{opt}} - \hat{n}^i_k$ stations should be redistributed to other RAW groups/slots evenly.
5: **Step 5:** Repeat step 3.

Algorithm 1: RAW adaption algorithm in RO-RAW.

If the number of competing stations is beyond the optimal value, some of the stations should be reallocated to other RAW groups. However, how to estimate the current competing stations is another problem to be solved.

3.2. Channel-State Estimation with Extended Kalman Filter. In order to estimate the current competing station number, we get inspiration from equation (7). If we measure the collision probability p, we can calculate the number of stations n by equation (7). Luckily, p can be simply measured by monitoring the channel state for each station. Specifically, one station can monitor the channel for all backoff slot times. If T is the total number of the observed slots, T_b is the number of busy slots sensed by the station (other stations are transmitting) and T_c is the number of collision slots (failed transmission for the station); it is obvious that p can be calculated as:

$$p = \frac{T_c + T_b}{T}. \tag{11}$$

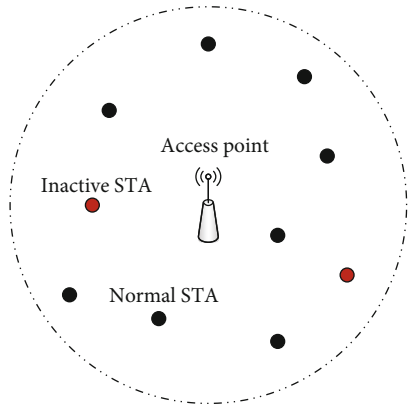

Figure 4: Example of the test topology.

Table 2: The parameters used in simulation.

PHY layer parameters	
Reception energy threshold	-116.0 dbm
Noise figure	3 db
Channel bandwidth	2 MHz
Data rate	2.4 Mbps
Maximal distance between AP and stations	250 m
MAC layer parameters	
$\mathrm{CW}_{\mathrm{min}}$	15
$\mathrm{CW}_{\mathrm{max}}$	1023
Traffic interval	0.1 s
Packet payload size	250/400 bytes
Number of groups	1
Algorithm parameters	
P_0	100
n_0	1
Q	0.6
R	1

Since the value of p is obtained, it is easy to calculate the instantaneous number of competing stations n. However, only the run-time estimation for a certain period can be really used by the optimization algorithms. We decide to adopt the Kalman filter to provide a run-time adaptive estimation of n. In fact, there are several simple estimation methods such as autoregressive and autoregressive moving average, but they are proven to be too simple to track the variations of the channel status accurately [22]. Thus, we decide to adopt the Kalman filter to provide a run-time adaptive estimation of n.

According to the definition of the network system, the system state can be represented by the following equations at discrete time k:

$$n_k = n_{k-1} + u_k, \tag{12}$$

$$p_k = y^{-1}(n_k) + v_k = h(n_k) + v_k. \tag{13}$$

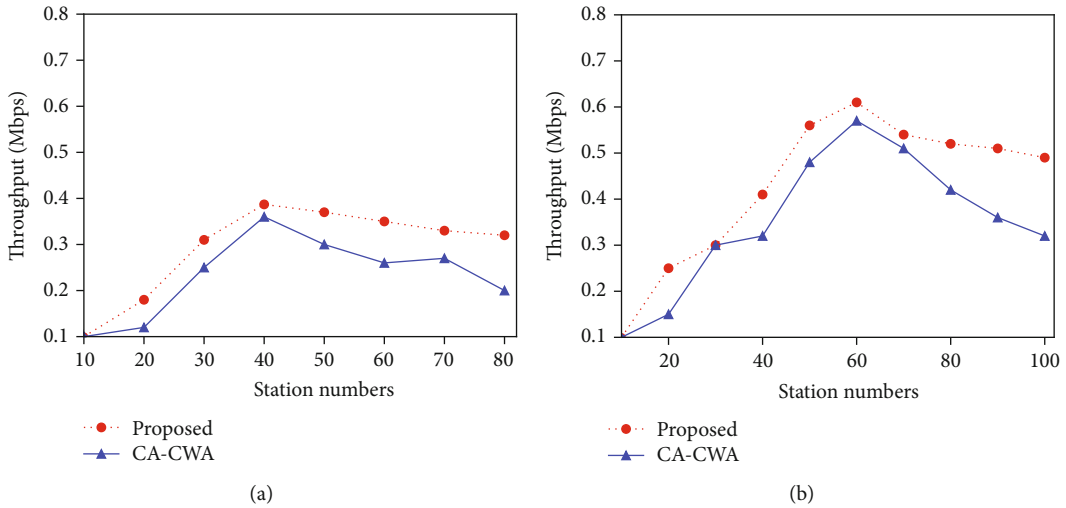

Figure 5: Performance of throughput of each scheme in the first scenario. (a) Throughput comparison when the payload size = 250 B, (b) Throughput comparison when the payload size = 400 B.

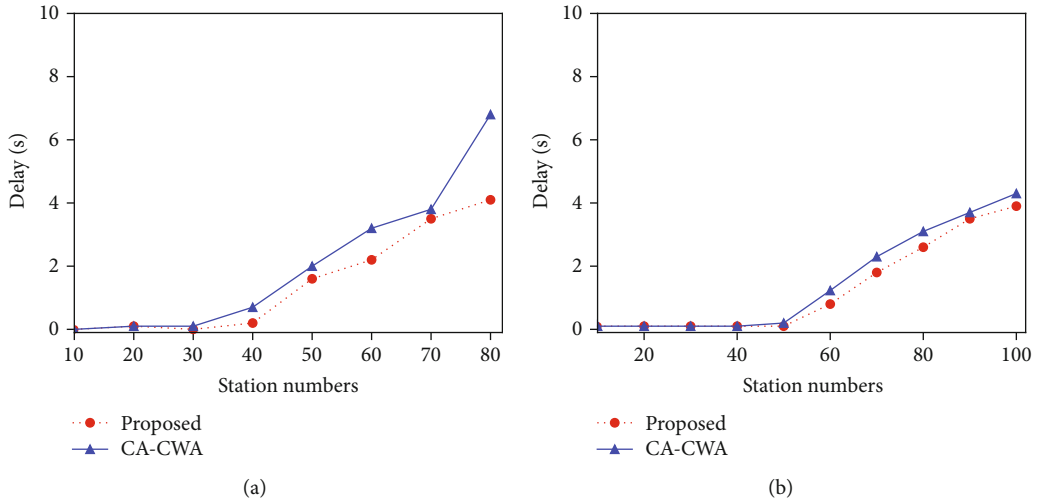

Figure 6: Performance of average delay of each scheme in the first scenario. (a) Average delay comparison when the payload size = 250 B, (b) Average delay comparison when the payload size = 400 B.

In equation (12), n_k stands for the number of stations at time k and v_k is the state random noise. This equation implies the approximate value of current n can be represented by the value of last state n plus a random variable. In equation (13), p_k is the collision probability at time k, and $y^{-1}(n_k)$ is the inverse function of equation (7). This equation means we can also obtain another approximate value of current n by measuring the collision probability.

Since the system state model is formulated, according to the general extended Kalman filter definition, it is easy to build the following iteration equations of the algorithm:

$$\hat{n}_k = \hat{n}_{k-1} + K_k z_k, \tag{14}$$

where K_k is the Kalman gain, and z_k is the measurement at time k. These two variables can be described by the following equations according to the definition:

$$z_k = p_k - \hat{h}(k-1), \tag{15}$$

$$K_k = \frac{(P_{k-1} + Q_k)h_k}{(P_{k-1} + Q_k)h_k^2 + R_k}. \tag{16}$$

In equation (16), Q_k and R_k are the variances of the random variable u_k and v_k, which are the noise in the updating process and measurement process, respectively. h_k is the

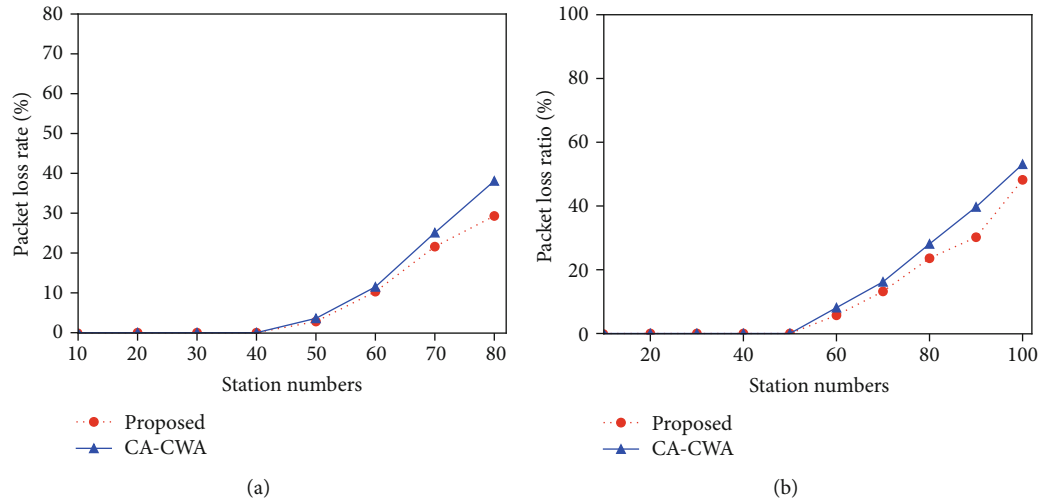

FIGURE 7: Performance of packet loss rate of each scheme in the first scenario. (a) Packet loss rate comparison when the payload size = 250 B, (b) Packet loss rate comparison when the payload size = 400 B.

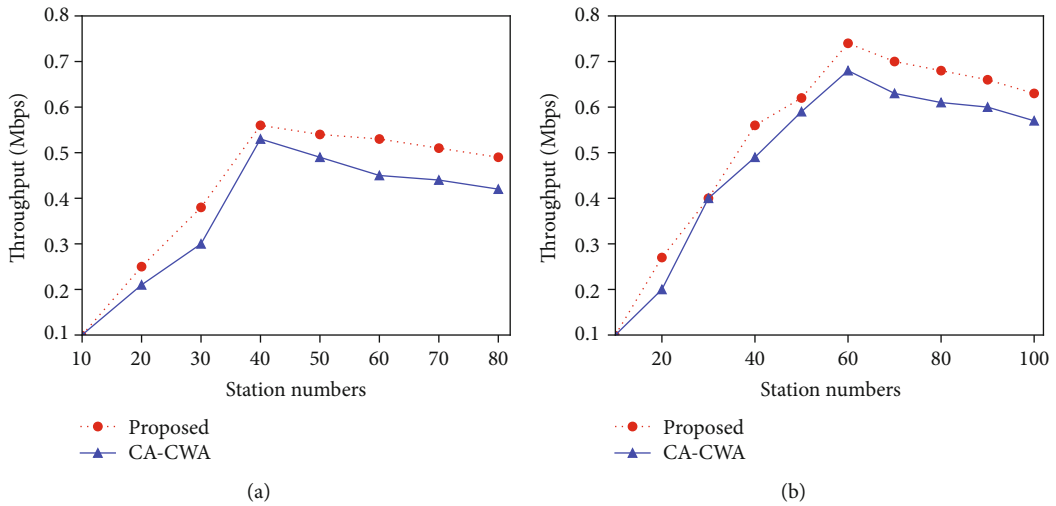

FIGURE 8: Performance of throughput of each scheme in the second scenario. (a) Throughput comparison when the payload size = 250 B, (b) Throughput comparison when the payload size = 400 B.

measurement sensitivity, which is linearized around the last estimated value n_{k-1}. It is calculated by taking the derivative:

$$h_k = \frac{\mathrm{d}h(n)}{\mathrm{d}n}. \tag{17}$$

The error variance of the new estimation can be calculated recursively:

$$P_k = (1 - K_k h_k)(P_{k-1} + Q_k). \tag{18}$$

In the last step to complete the design of the EKF-based estimation method, it remains to specify several parameters including the state noise Q and R, which affects the convergence rate of the estimator to some extent. According to the general applications of the Kalman filter, Q and R are usually given the constant values. Thus, these parameters are given by simple tests in this paper. We set $Q = 0.6$, $R = 1$, and $P_0 = 100$ for relatively quick convergence performance. A more accurate parameter analysis and optimization are beyond the scope of this paper. Based on the EKF-based run-time channel state estimation method, it is simple to adjust the RAW parameters according to the estimated number of current competing stations $\hat{n}_k$.

3.3. RAW Adaption Algorithm. As discussed in Section 3.1, there exists a competing station number n_{opt} to optimize the network performance in each RAW slot. Since the number of current competing stations is obtained from the method introduced in Section 3.2, it is easy to adjust the RAW parameters to reallocate the distribution of the stations. Specifically, all stations should observe the channel for the total backoff period and estimate the number of active stations by the method introduced in Section 3.2. If the

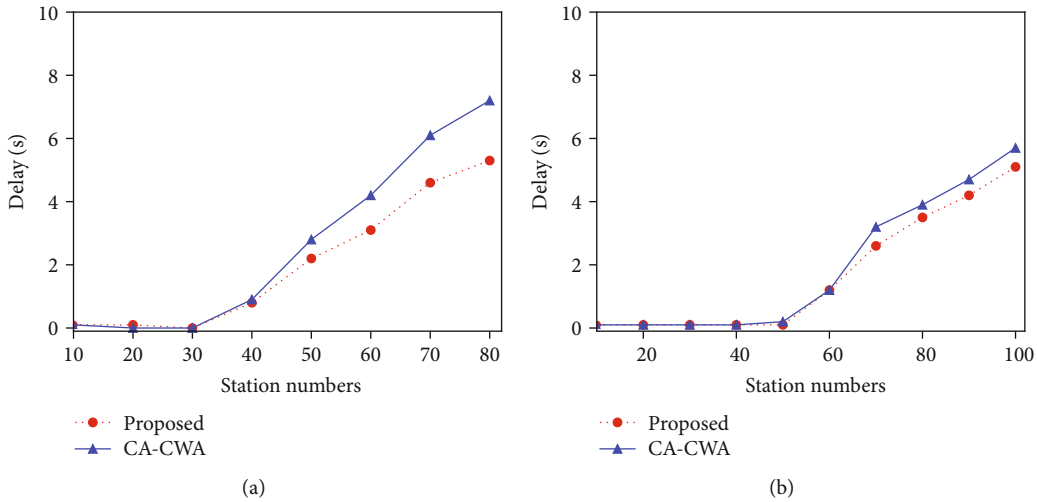

Figure 9: Performance of the average delay of each scheme in the second scenario. (a) Average delay comparison when the payload size = 250 B, (b) Average delay comparison when the payload size = 400 B.

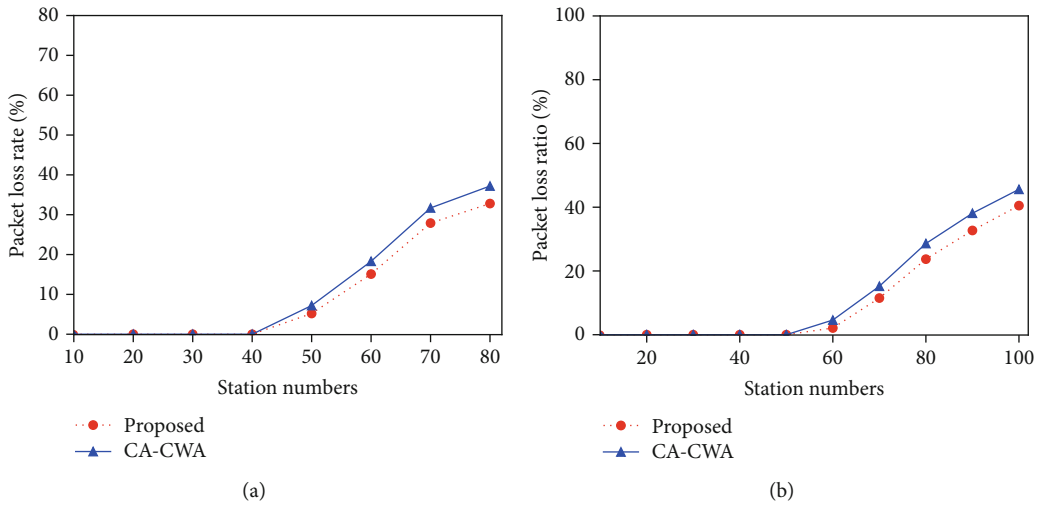

Figure 10: Performance of the packet loss rate of each scheme in the second scenario. (a) Packet loss rate comparison when the payload size = 250 B, (b) Packet loss rate comparison when the payload size = 400 B.

estimated value $\hat{n}_k$ is beyond the value of n_{opt} for a period T_p, then the active stations should be reallocated to other RAW groups evenly. Otherwise, the RAW group allocation should not be changed. The process of the RAW adaption algorithm is summarized in Algorithm 1.

4. Performance Evaluation

In this section, we present the simulation results and corresponding analysis to demonstrate the performance of the proposed RO-RAW scheme in the IEEE 802.11ah networks.

4.1. Simulation Setup. All the evaluations are performed in the NS-3 simulator with the 802.11ah module, which is proposed in [23, 24]. The simulation is based on a typical WLAN scenario, where one AP is located in the center, and other stations are distributed around the AP randomly. 10% of the stations are set inactive (associate with AP but transmit almost no data). The test topology example is given in Figure 4. In the simulation, the DCF parameters, including CW_{min} and CW_{max}, are set to the default values. Other PHY and MAC network parameters used in the simulation are shown in Table 2. Besides, in the algorithm design, initial iteration values have a significant impact on the convergence speed of the algorithm. In the simulation, we set $P_0 = 100$ and $n_0 = 1$ for quick convergence. The other algorithm parameters used in the simulation are also listed in Table 2.

The performance of the RAW mechanism can be evaluated in terms of three metrics: throughput, delay, and packet loss rate. Throughput is computed by the average received payload bytes by the AP per second. Delay is obtained by measuring the average time a packet experienced between the sender and the receiver. The packet loss is calculated by counting the number of packets not received, and the total

number of packets sent. Each simulation runs 300 s, which is enough to show the performance of the proposed RAW optimization scheme. Besides, to improve the reliability of the simulation results, each simulation was conducted five times, and the final results are the average of the five. The proposed RAW adaption scheme is compared with another RAW optimization scheme CA-CWA, which is also based on the channel status estimation. However, CA-CWA just tunes the contention window to improve the network performance, while RO-RAW adjusts the number of stations in a different RAW period.

4.2. Simulation Results. In the simulation, to validate the effectiveness of the proposed algorithms more precisely, the simulation is conducted in two simulation scenarios for two different RAW configurations. In the first scenario, the slot format subfield is filled with 1, and the RAW slots and C is set to 4 and 200. This configuration provides less slots in a RAW period, but a longer time for each slot.

Figures 5(a) and 5(b) show the throughput performance of the two RAW optimization schemes when varying the number of RAW stations. We observed that the network throughput associated with each algorithm increased as the number of RAW stations n increased until a maximum point ($n = 40$ in Figure 5(a) and $n = 50$ in Figure 5(b)), and the value begins to decline. It is the basic RAW throughput characteristics which has been proved in several researches [9, 25]. Figures 5(a) and 5(b) further show that RO-RAW has better performance on throughput than CA-CWA. We take the simulation results in Figure 5(a) for example. No matter how the number of nodes changes, RO-RAW has better performance than CA-CWA. However, after the throughput reaches the peak value ($n > 40$), RO-RAW has a more significant performance improvement. It is because CA-CWA is a contention window-based optimization scheme, which can only adjust the contention window of the station. But it cannot adjust the distribution of the stations in each RAW period and RAW slot. It means the load distribution of the stations is perhaps not balanced, and this issue may be worse when the number of inactive nodes is large. RO-RAW overcomes this problem and thus achieves a better performance.

Figures 6(a) and 6(b) illustrate the delay performance of the two RAW optimization schemes when varying the number of RAW stations. It can be observed that when the station numbers are relatively low ($n = 40$ in Figure 6(a) and $n = 50$ in Figure 6(b)), the average delay is almost zero. The reason is that the channel competition is not very severe in these cases. But when the number of stations gets higher, there is a significant increase in the average delay due to the severe channel competition. Figures 6(a) and 6(b) further show that our proposed scheme also has better performance on average delay than CA-CWA. When the channel gets crowded, RO-RAW is able to estimate the channel status and reallocated the RAW slots. Thus, it has a better delay performance when the number of stations is relatively higher compared with CA-CWA. The same conclusion can be also drawn when analyzing the packet loss performance (Figures 7(a) and 7(b)) of the two schemes.

In the second scenario, the slot format subfield is filled with 0, and the RAW slots and C are set to 8 and 50. This configuration provides a larger number of slots in a RAW period, but a shorter time for each slot, compared with the first scenario. However, the main conclusions are similar to the conclusions obtained in the first scenario.

As shown in Figures 8(a) and 8(b), the peak value and other values are changed compared with the values in the first scenario because the number of the RAW slots has been increased and the value of C is decreased. But the general trend of the throughput curve does not change. RO-RAW still shows its performance advantages than CA-CWA, especially when the number of stations is relatively large. The same conclusion can be also drawn when analyzing the delay (Figures 9(a) and 9(b)) and packet loss performance (Figures 10(a) and 10(b)) of the two schemes in the second scenario.

5. Conclusion

In this paper, we propose a run-time RAW optimization scheme with the extended Kalman filter, namely, RO-RAW, to improve the RAW performance in IEEE 802.11ah networks. RO-RAW first estimates the current channel status and returns the estimated station numbers by the EKF method. Based on the estimated number of competing stations, RO-RAW adjusts the RAW parameters to the optimal parameter settings which are calculated in advance. To validate the performance of the proposed scheme, we compared it with another RAW optimization scheme CA-CWA in the NS-3 simulator. The simulation results show that RO-RAW substantially improves the throughput, latency, and packet loss performance compared with CA-CWA in different simulation scenarios. The results further show that, when the channel is relatively congested, RO-RAW improves the performance of RAW more significantly.

Data Availability

The data used to support the findings of this study are included in the article.

Conflicts of Interest

The authors declare that they have no conflicts of interest.

Acknowledgments

This work was supported by the Major National Science and Technology Program of China: High-Grade Numerical Control Machine Tools and Basic Manufacturing Equipment (No. 2019ZX04003001-006).

References

[1] Y. Cheng, Y. Zhang, P. Ji, W. Xu, Z. Zhou, and F. Tao, "Cyber-physical integration for moving digital factories forward towards smart manufacturing: a survey," *The International Journal of Advanced Manufacturing Technology*, vol. 97, no. 1-4, pp. 1209–1221, 2018.

[2] M. Sharp, R. Ak, and T. Hedberg Jr., "A survey of the advancing use and development of machine learning in smart

manufacturing," *Journal of Manufacturing Systems*, vol. 48, pp. 170–179, 2018.

[3] R. Masoni, F. Ferrise, M. Bordegoni et al., "Supporting remote maintenance in industry 4.0 through augmented reality," *Procedia Manufacturing*, vol. 11, pp. 1296–1302, 2017.

[4] C. Zhao, N. Kang, J. Li, and J. A. Horst, "Production control to reduce starvation in a partially flexible production-inventory system," *IEEE Transactions on Automatic Control*, vol. 63, no. 2, pp. 477–491, 2018.

[5] M. Chui, M. Miremadi, J. Bughin, K. George, P. Willmott, and M. Dewhurst, "A future that works: Ai, automation, employment, and productivity," vol. 60, McKinsey Global Institute Research, Technical Report, 2017.

[6] Y. Cheng, D. Yang, and H. Zhou, "Det-WiFi: a multihop TDMA MAC implementation for industrial deterministic applications based on commodity 802.11 hardware," *Wireless Communications and Mobile Computing*, vol. 2017, Article ID 4943691, 10 pages, 2017.

[7] Y. Cheng, D. Yang, H. Zhou, and H. Wang, "Adopting IEEE 802.11 MAC for industrial delay-sensitive wireless control and monitoring applications: a survey," *Computer Networks*, vol. 157, pp. 41–67, 2019.

[8] V. Baños-Gonzalez, M. S. Afaqui, E. Lopez-Aguilera, and E. Garcia-Villegas, "IEEE 802.11ah: a technology to face the IoT challenge," *Sensors*, vol. 16, no. 11, p. 1960, 2016.

[9] O. Raeesi, J. Pirskanen, A. Hazmi, T. Levanen, and M. Valkama, "Performance evaluation of IEEE 802.11ah and its restricted access window mechanism," in *2014 IEEE International Conference on Communications Workshops (ICC)*, pp. 460–466, Sydney, NSW, Australia, 2014.

[10] E. Khorov, A. Krotov, and A. Lyakhov, "Modelling machine type communication in IEEE 802.11ah networks," in *2015 IEEE International Conference on Communication Workshop (ICCW)*, pp. 1149–1154, London, UK, 2015.

[11] M. Z. Ali, J. Misic, and V. B. Misic, "Performance evaluation of heterogeneous IoT nodes with differentiated QoS in IEEE 802.11ah RAW mechanism," *IEEE Transactions on Vehicular Technology*, vol. 68, no. 4, pp. 3905–3918, 2019.

[12] T. Sakurai and H. L. Vu, "MAC access delay of IEEE 802.11 DCF," *IEEE Transactions on Wireless Communications*, vol. 6, no. 5, pp. 1702–1710, 2007.

[13] T. Adame, A. Bel, B. Bellalta, J. Barcelo, and M. Oliver, "IEEE 802.11AH: the wifi approach for M2M communications," *IEEE Wireless Communications*, vol. 21, no. 6, pp. 144–152, 2014.

[14] W. Sun, M. Choi, and S. Choi, "IEEE 802.11 ah: a long range 802.11 WLAN at sub 1 GHz," *Journal of ICT Standardization*, vol. 1, no. 1, pp. 83–108, 2017.

[15] E. Khorov, A. Lyakhov, A. Krotov, and A. Guschin, "A survey on IEEE 802.11ah: an enabling networking technology for smart cities," *Computer Communications*, vol. 58, pp. 53–69, 2015.

[16] T.-C. Chang, C.-H. Lin, K. C.-J. Lin, and W.-T. Chen, "Traffic-aware sensor grouping for IEEE 802.11ah networks: regression based analysis and design," *IEEE Transactions on Mobile Computing*, vol. 18, no. 3, pp. 674–687, 2019.

[17] C. W. Park, D. Hwang, and T.-J. Lee, "Enhancement of IEEE 802.11ah MAC for M2M communications," *IEEE Communications Letters*, vol. 18, no. 7, pp. 1151–1154, 2014.

[18] Y. Cheng, H. Zhou, and D. Yang, "Ca-CWA: channel-aware contention window adaption in IEEE 802.11ah for soft real-time industrial applications," *Sensors*, vol. 19, no. 13, p. 3002, 2019.

[19] G. Bianchi, "Performance analysis of the IEEE 802.11 distributed coordination function," *IEEE Journal on Selected Areas in Communications*, vol. 18, no. 3, pp. 535–547, 2000.

[20] G. Bianchi and I. Tinnirello, "Remarks on IEEE 802.11 DCF performance analysis," *IEEE Communications Letters*, vol. 9, no. 8, pp. 765–767, 2005.

[21] G. Bianchi and I. Tinnirello, "Kalman filter estimation of the number of competing terminals in an IEEE 802.11 network," in *IEEE INFOCOM 2003. Twenty-second Annual Joint Conference of the IEEE Computer and Communications Societies (IEEE Cat. No.03CH37428)*, vol. 2, pp. 844–852, San Francisco, CA, USA, 2003.

[22] I. Tinnirello and A. Sgora, "A Kalman filter approach for distinguishing channel and collision errors in IEEE 802.11 networks," in *IEEE GLOBECOM 2008-2008 IEEE Global Telecommunications Conference*, pp. 1–5, New Orleans, LO, USA, 2008.

[23] L. Tian, S. Deronne, S. Latré, and J. Famaey, "Implementation and validation of an IEEE 802.11 ah module for ns-3," in *Proceedings of the Workshop on ns-3*, pp. 49–56, Seattle WA USA, 2016.

[24] L. Tian, A. Šljivo, S. Santi, E. De Poorter, J. Hoebeke, and J. Famaey, "Extension of the IEEE 802.11 ah ns-3 simulation module," in *Proceedings of the 10th Workshop on ns-3*, pp. 53–60, Surathkal India, 2018.

[25] L. Tian, J. Famaey, and S. Latré, "Evaluation of the IEEE 802.11ah restricted access window mechanism for dense IoT networks," in *2016 IEEE 17th International Symposium on A World of Wireless, Mobile and Multimedia Networks (WoWMoM)*, pp. 1–9, Coimbra, Portugal, 2016.